

Received August 17, 2019, accepted September 5, 2019, date of publication September 12, 2019, date of current version September 25, 2019.

Digital Object Identifier 10.1109/ACCESS.2019.2940723

Determination of Complex Permittivity of Low-Loss Materials From Reference-Plane Invariant Transmission/Reflection Measurements

CHUANG YANG^{1,2,3} AND HUI HUANG⁴, (Member, IEEE)

¹School of Microelectronics, Tianjin University, Tianjin 300072, China

²Qingdao Key Laboratory of Ocean Perception and Information Transmission, Qingdao 266200, China

³Qingdao Institute for Ocean Technology of Tianjin University, Qingdao 266200, China

⁴Xinchen Technology Company Ltd., Beijing 100029, China

Corresponding author: Chuang Yang (chuangyang@tju.edu.cn)

This work was supported by the National Key R&D Program of China under Grant 2016YFA0202200.

ABSTRACT In this paper, a novel method is proposed to determine unique and stable relative complex permittivity of low-loss materials from the transmission/reflection (TR) measurements, though the positions of the materials under test are unknown. The proposed method systematically combines artificial neural network (ANN) models with the Nicolson-Ross-Weir (NRW) method. Firstly, an ANN model is established to estimate the position of the sample in the transmission line. Secondly, the NRW method is adapted to estimate the relative complex permittivity, and the unique solutions are selected with the help of dielectric properties. Thirdly, the noniterative technique in the literature is adapted to avoid the instabilities in the relative complex permittivity. Finally, the S -parameters of the amplitude-only or transmission-only measurements are used to accurately determine the relative complex permittivity. The proposed method is experimentally validated by two samples. The simulated data are used to further validate the accuracy of the proposed method. The results of the proposed method based on the transmission-only measurements are the most accurate.

INDEX TERMS Complex permittivity, transmission/reflection, position-unknown, reference-plane invariant.

I. INTRODUCTION

Precise knowledge on electromagnetic properties of materials is a fundamental requisite for engineering design of electrical systems. Determination of relative complex permittivity (ϵ_r) of materials at microwave frequencies is necessary for microwave engineering [1], [2]. To date, various determination methods, each with its own advantages and constraints, have been proposed. Among these methods, the methods based on the transmission/reflection (TR) measurements are widely adopted for determination of ϵ_r since they are broadband and easy to be carried out [3], [4]. However, the methods based on the TR measurements have three main drawbacks [5], which need to be eliminated. First, there are always multiple solutions which arise from the ambiguity in phase of the transmitted field (S_{21}) [6]–[8]. Second, the determined ϵ_r of low-loss materials at frequencies corresponding

to integer multiples of one-half wavelength in the sample are unstable [9]. That is mainly caused by the large phase uncertainty of the reflection parameters (S_{11} and S_{22}) at those frequencies [3], [4], [9], [10]. Especially at high frequencies, the wavelength is so short that this drawback is hard to be avoided. The third drawback occurs when the reference planes (calibration planes) and the measurement planes (planes at sample end surfaces) do not meet [5]. Therefore, any uncertainty of sample position in its holder causes serious measurement errors [5]. Unfortunately, the position of the sample can be shifted in the course of connecting or disconnecting the sample holder with the vector network analyzer (VNA) connectors [11].

For decades, lots of techniques have been introduced to eliminate these drawbacks. Various techniques have been discussed to eliminate the drawback of multiple solutions, such as the group-delay technique [6], the multiple phase measurements approach [12], the amplitude-only method [13]–[15], the Kramers–Kronig relations method [8], [16], the stepwise

The associate editor coordinating the review of this manuscript and approving it for publication was Datong Liu.

technique [17], and the phase-unwrapping technique [18]. Techniques for eliminating or suppressing the instabilities have also been presented, such as the noniterative technique [9], the multiple-thickness approach [3], the approximation techniques [19], [20], the Baker-Jarvis iterative techniques [21], [22], and the short-circuit method [10]. While various reference-plane-invariant methods have been proposed to avoid the effects of position on the determination of ϵ_r [23]–[27]. In addition, there are methods which have the ability to eliminate the three drawbacks all at once, such as the amplitude-only [26] and the transmission-only [27] methods. However, both of the methods need a good initial guess.

Recently, Hasar [5] proposed a method without initial guesses for removing the aforementioned three drawbacks all at once. However, two shorted-reflection and one transmission S -parameters are measured in the method that increases the uncertainty of the determined ϵ_r as the measured S -parameters are the main sources of errors in the extracted ϵ_r [28]. In addition, the calculation formulars are so complicated.

In this paper, a simple method is proposed to eliminate the three drawbacks all at once. The method contains several but simple steps. Firstly, an artificial neural network (ANN) model is established to estimate the position of the sample in the transmission line. Secondly, NRW method [6] is adopted to roughly estimate ϵ_r since the position is the estimated value, and the unique solutions are selected since only the dielectric material is tested in this paper. Thirdly, the noniterative stable technique [9] is adopted to avoid the instabilities in the ϵ_r . Finally, the nonlinear-least-squares-type fitting (NLSTF) technique [10] is applied. The amplitude-only measured S -parameters or the transmission-only measured S -parameters are used to determine the ϵ_r with the help of the abovementioned estimated results. In addition, the method using the transmission-only measured S -parameters is more accurate than the method using the amplitude-only measured S -parameters. Because the uncertainties of the measured $|S_{11}|$ are large at the Fabry-Perot frequencies as illustrated in [10]. Therefore, the values of the ϵ_r extracted by the proposed method are only related to the measured S_{21} (or the measured $|S_{11}|$ and $|S_{21}|$) and the length of the sample. There are no complicated calculations in the proposed method. The experimental results of two samples are performed to validate the proposed method.

The paper is organized as follows. In Section II, we present the proposed method in detail. The experiments and discussion are shown to validate the proposed method in Section III. In Section IV, the simulations and discussion are shown to validate the accuracy of the proposed method. In Section V, we conclude the whole paper.

II. METHOD

Fig. 1 shows a sample positioned arbitrarily inside a transmission line with length of L_0 . The sample is a low-loss dielectric material with length of L . The values of L_{01} and L_{02} are unknown. Usually, the S -parameters between the Port 1

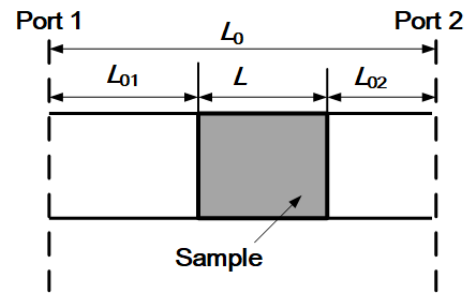


FIGURE 1. A transmission line containing a sample for the TR measurements. The L_{01} and L_{02} are unknown. The transmission line could be a waveguide or a coaxial line.

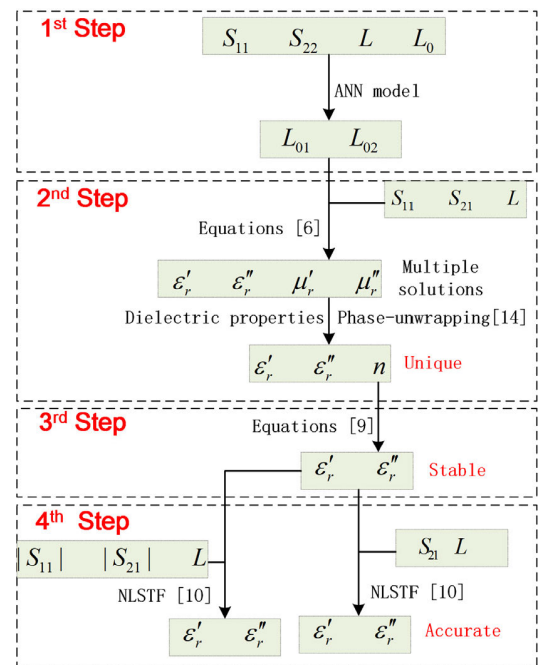


FIGURE 2. Processes for a low-loss material complex permittivity determination. The results are unique, stable, accurate and position-independent.

and Port 2 are measured to determine the ϵ_r of the sample. The processes of the proposed method for determining the ϵ_r of the sample are shown in Fig. 2. The proposed method is equally applicable to waveguide and coaxial measurements, though the examples discussed herein are performed in a waveguide. There are four steps in the proposed method to eliminate the three drawbacks. We present the processes in detail as follows.

A. POSITION ESTIMATION USING ANN

The aim of this step is to estimate the values of L_{01} and L_{02} . According to [3], we can express the theoretical S -parameters between the Port 1 and Port 2 in Fig. 1 as

$$S_{11} = R_{01}^2 \frac{\Gamma(1 - T^2)}{1 - \Gamma^2 T^2} \tag{1}$$

$$S_{21} = S_{12} = R_{01} R_{02} \frac{T(1 - \Gamma^2)}{1 - \Gamma^2 T^2} \tag{2}$$

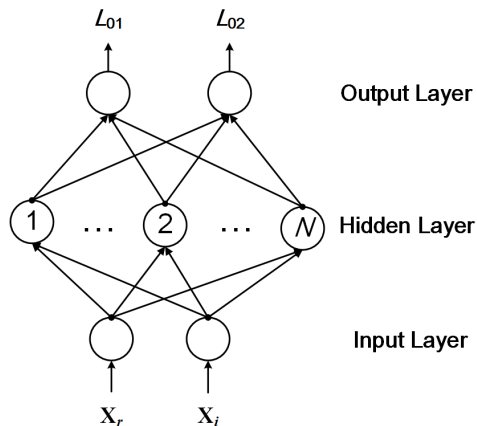


FIGURE 3. The structure of the ANN model used for position estimation.

$$S_{22} = R_{02}^2 \frac{\Gamma(1 - T^2)}{1 - \Gamma^2 T^2} \quad (3)$$

where

$$R_{01} = e^{-\gamma_0 L_{01}} \quad (4)$$

$$R_{02} = e^{-\gamma_0 L_{02}} \quad (5)$$

$$\Gamma = \frac{\gamma_0 - \gamma}{\gamma_0 + \gamma} \quad (6)$$

$$T = e^{-\gamma L} \quad (7)$$

$$\gamma = j \sqrt{\frac{\omega^2 \epsilon_r \mu_r}{c_{vac}^2} - \left(\frac{2\pi}{\lambda_c}\right)^2} \quad (8)$$

$$\gamma_0 = j \sqrt{\frac{\omega^2}{c_{lab}^2} - \left(\frac{2\pi}{\lambda_c}\right)^2} \quad (9)$$

In these equations, γ_0 and γ are the propagation constants in the air-filled and the sample-filled regions inside the waveguide. T is the propagation factor for a wave propagating through the sample. Γ is the reflection coefficient at the interface between the air-filled waveguide and sample-filled waveguide when the sample is infinite. R_{01} and R_{02} are the propagation factors of the air-filled waveguide. λ_c is the cut-off wavelength of the waveguide. c_{vac} and c_{lab} are the speed of light in vacuum and laboratory. ω is the angular frequency. $\epsilon = \epsilon_0 \epsilon_r = \epsilon_0 (\epsilon_r' - j\epsilon_r'')$ is the complex permittivity of the sample, and $\mu = \mu_0 \mu_r = \mu_0 (\mu_r' - j\mu_r'')$ is the complex permeability of the sample.

According to (1), (3)-(5), we can derive a function

$$X = X_r + jX_i = \frac{S_{11}}{S_{22}} = \frac{R_{01}^2}{R_{02}^2} = e^{-2\gamma_0(L_{01} - L_{02})} \quad (10)$$

where L_{01} ranges from 0 to $L_0 - L$, L_{02} ranges from 0 to $L_0 - L$, and $L_0 = L + L_{01} + L_{02}$.

In order to determine the values of L_{01} and L_{02} , we propose an ANN-based method. The structure of the ANN model is shown in Fig. 3. The inputs of the model are X_r and X_i . The outputs of the ANN model are L_{01} and L_{02} . The values of L_{01} and L_{02} have been used to calculate the X_r and X_i

from (9) and (10). In the ANN model, there are N hidden nodes and the back-propagation algorithm is used. Once the model has been trained, the testing data are used to verify the ANN model by the Mean Square Error (MSE) [29]. Only if the value of the MSE approaches 10^{-6} or even lower for the testing data, the trained ANN model will be considered accurate. Otherwise, the parameters should be retrained by adjusting the value of N .

In the end, the X_r and X_i calculated from the measured S_{11} and S_{22} are put into the trained ANN model. The outputs of the trained ANN model are the values of L_{01} and L_{02} .

B. PHASE AMBIGUITY ELIMINATION BASED ON DIELECTRIC PROPERTIES

In this step, we propose a simple technique to determine the unique ϵ_r . After position estimation, the ϵ_r is calculated from the follow equations [9], which also can be derived from (1)-(9)

$$\frac{1}{\Lambda^2} = - \left[\frac{1}{2\pi L} \ln\left(\frac{1}{T}\right) \right]^2 = - \left[\frac{1}{2\pi L} \ln\left(\left|\frac{1}{T}\right|\right) + \frac{j\phi}{2\pi L} + \frac{jn}{L} \right]^2, \quad n = 0, \pm 1, \pm 2, \dots \quad (11)$$

$$\mu_r = \frac{1 + \Gamma}{\Lambda(1 - \Gamma) \sqrt{\frac{1}{\lambda_0} - \frac{1}{\lambda_c}}} \quad (12)$$

$$\epsilon_r = \frac{\lambda_0^2 \left(\frac{1}{\Lambda^2} + \frac{1}{\lambda_c}\right)}{\mu_r} \quad (13)$$

In (11)-(13), Γ and T can be calculated from the measured S -parameters by the NRW method [6].

The integer n in (11) has an infinite number of solutions, that is caused by the well-known phase ambiguity [17], [18]. The value of n has large effects on real part of $1/\Lambda$, therefore the value of relative complex permeability μ_r changes with the change of n . As the measured sample is a dielectric, μ_r should be equal to 1. The value of n is correct when $\mu_r \rightarrow 1$. We only determine the value of n at some frequencies far away from Fabry-Perot frequencies, because the calculated μ_r around Fabry-Perot frequencies is resonant and inaccurate [5]. According to the determined n at some frequencies, the values of n at other frequencies are determined by the phase-unwrapping technique [18], which is easy to be performed. After n is determined, Λ is unique. Then, the phase ambiguity is eliminated in the whole frequency range.

C. INSTABILITY ELIMINATION

The Λ determined in the last step is adopted in this section. When the μ_r of dielectric materials equals to 1, (13) can be further simplified. The stable relative complex permittivity is expressed as [9]

$$\epsilon_r = \lambda_0^2 \left(\frac{1}{\Lambda^2} + \frac{1}{\lambda_c} \right). \quad (14)$$

TABLE 1. Summaries for advantages and disadvantages of the different methods.

| Method | Classical | | | Removing the three drawbacks | | |
|---------------------------|--------------------------------|--------------------|----------------------|------------------------------|-------------------------|--|
| | [6] | [9] | [13] | [27] | [5] | This work |
| Variables for calculation | $ S_{11} $ | √ | √ | √ | — | — |
| | $\varphi(S_{11})$ | √ | √ | — | — | — |
| | $ S_{21} $ | √ | √ | √ | √ | √ |
| | $\varphi(S_{21})$ | √ | √ | — | √ | √ |
| | $ S_{11s} $ | — | — | — | — | √ |
| | $\varphi(S_{11s})$ | — | — | — | — | √ |
| | $ S_{22s} $ | — | — | — | — | √ |
| | $\varphi(S_{22s})$ | — | — | — | — | √ |
| | L | √ | √ | √ | √ | √ |
| | L_{01} | √ | √ | — | — | — |
| Advantages | Unique | Unique | Stable | Stable | Unique | Unique |
| | | Stable | Position-Independent | Position-Independent | Stable | Stable |
| Disadvantages | Unstable Position-dependent | Position-dependent | Initial guess | Initial guess | Complicated calculation | — |
| | | — | — | — | Position-Independent | Position-Independent Simple calculation |

√: The variable exists; —: The variable does not exist. $\varphi(S_{11})$ is the phase of S_{11} , $\varphi(S_{21})$ is the phase of S_{21} , $\varphi(S_{11s})$ is the phase of S_{11s} , $\varphi(S_{22s})$ is the phase of S_{22s} .

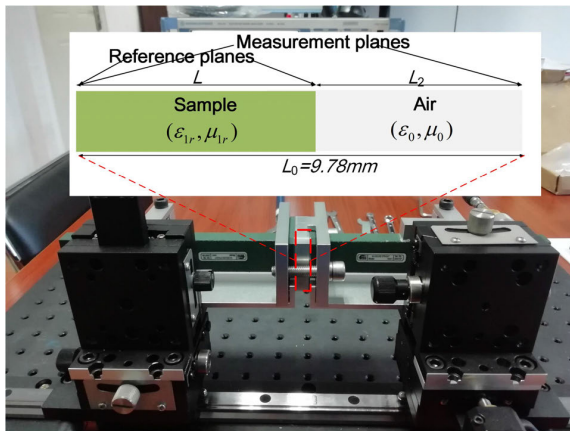


FIGURE 4. Photograph of measurement setup and layout of a sample in the waveguide.

Baker-Jarvis *et al.* [22] explain that in the low-loss limit, a product of $\epsilon_r \mu_r$ is stable. In (14), $\epsilon_r = \epsilon_r \mu_r$. That explains why the extracted ϵ_r is stable.

D. ACCURATE DETERMINATION OF COMPLEX PERMITTIVITY

Up to now, the determined ϵ_r is not accurate due to that the position of the sample is the estimated value. In this section, the effects of the position are removed. That increases the accuracy of the determined ϵ_r . According to (1) and (2), we can see that $|S_{11}|$, $|S_{21}|$ and phase of S_{21} are independent of the position. Then, the results extracted from the three parameters are more accurate. Two processes can be used as shown in the 4th step in Fig. 2. We adopt the ϵ_r determined in the 3rd as the initial guess. The objective function to be minimized for a NLSTF is given as

$$f(\epsilon'_r, \epsilon''_r) = \left(|S_{21}^{meas}| - |S_{21}^{pred}| \right)^2 + \left(\frac{\angle S_{21}^{meas} - \angle S_{21}^{pred}}{180} \right)^2 \tag{15}$$

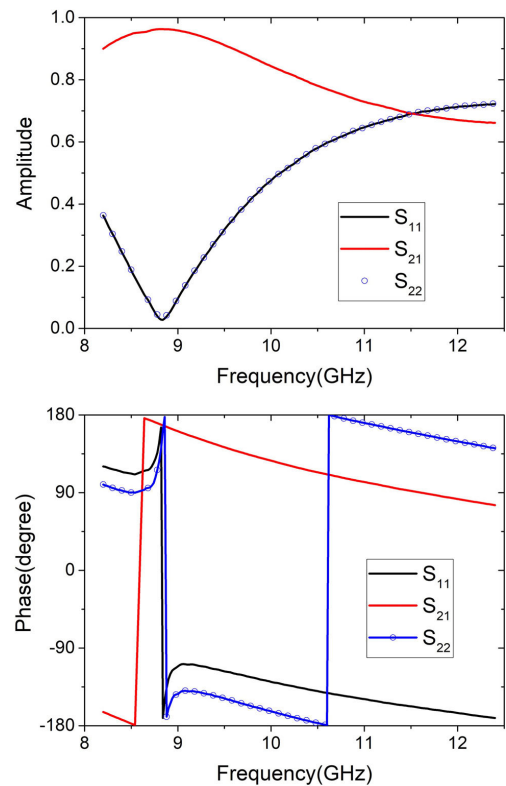


FIGURE 5. Two-port measured S-parameters results for the FR-4.

where the superscripts “meas” and “pred” refer to the measured and predicted values, respectively [10]. Another objective function to be minimized for a NLSTF is given as

$$f(\epsilon'_r, \epsilon''_r) = \left(|S_{11}^{meas}| - |S_{11}^{pred}| \right)^2 + \left(|S_{21}^{meas}| - |S_{21}^{pred}| \right)^2 \tag{16}$$

The advantages and disadvantages of the proposed method can be illustrated by the comparison in Table 1. The method in [6] is unstable and position-dependent; the method in [9]

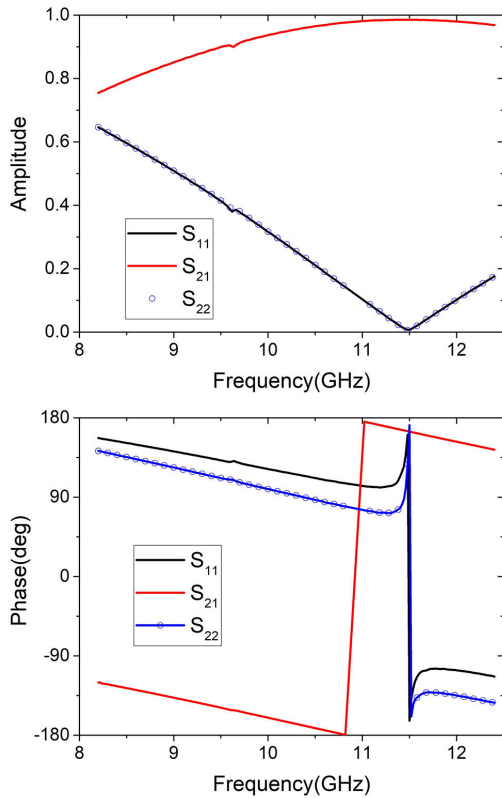


FIGURE 6. Two-port measured S-parameters results for the PVC.

TABLE 2. Estimation and measurement of the sample position.

| Sample | Estimation | | Measurement | |
|--------|---------------|---------------|---------------|---------------|
| | L_{01} (mm) | L_{02} (mm) | L_{01} (mm) | L_{02} (mm) |
| FR4 | -0.0147 | 1.8547 | 0 | 1.84 |
| PVC | 0.0199 | 1.2501 | 0 | 1.27 |

is position-dependent; the methods in [13] and [27] need a good initial guess; the method in [5] has a complicated calculation. The proposed technique is unique, stable and position independent. Compared with the method in [5], the proposed technique has a simple calculation.

III. EXPERIMENTS AND RESULTS

In this section, we use the experimental results to validate the proposed method. The experimental setup and the calculation process are shown as follows.

A. EXPERIMENTAL SETUP

The S-parameters for determining ϵ_r are measured with a two-port VNA (Rohde & Schwarz ZVA40). The ports of the VNA are connected to X-band coaxial-to-waveguide adapters to set up the measurement system as shown in Fig. 4. The system is calibrated in the X-band (8.2–12.4 GHz) with the standard thru-reflect-line (TRL) method. The sample holder is a rectangular waveguide operating at the X-band with length of $L_0 = 9.78$ mm.

B. MEASUREMENTS AND RESULTS

As shown in Fig. 4, the X-band rectangular waveguide shim with a sample is inserted between the two ports of

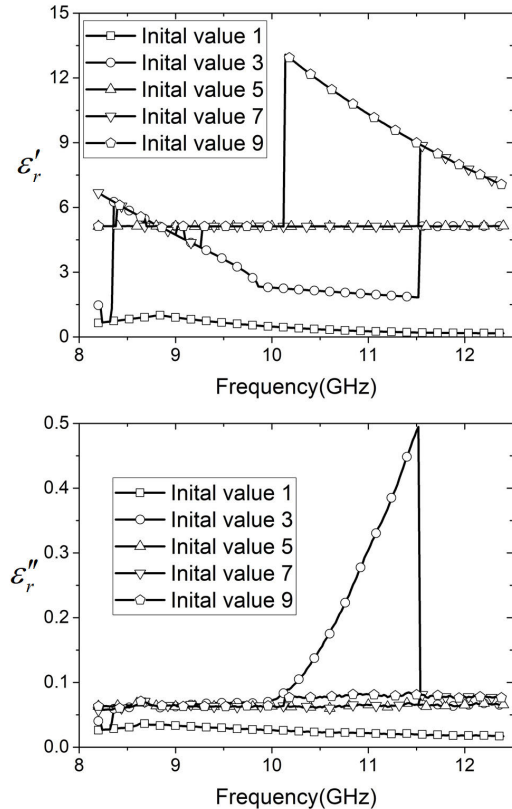


FIGURE 7. Determined relative complex permittivity of the FR-4 using Eq. (16), with various initial values for the start of the NLSTF.

the adapters. The processes of sample placement contain two steps: 1) place the short kit on the left side of the container (connecting to port 1) and insert the sample from right side of the container (connecting to port 2); 2) squeeze the sample from the right side of the container until it touches the short kit. The layout of a sample in the waveguide is also shown in Figure 4. The measured L_{01} and L_{02} are 0 and $L_0 - L$, respectively. We fabricated two low-loss samples (a FR4 sample with length of 7.94mm, and a PVC with length of 8.51mm) to validate the proposed method and compare its performances with other non-iterative methods [6], [9]. The measured S-parameters are shown in Fig. 5 and Fig. 6. For the FR-4 sample and the PVC sample, there are dips for the measured $|S_{11}|$ and peaks for the measured $|S_{21}|$ caused by Fabry-Perot resonances.

As shown in Table 2, the estimated positions of the samples approximate the measured positions. That is to say, the proposed position estimation method is effective. The length L_{01} and L_{02} are nonnegative values in (10), but the calculated results have negative value in Table 2. That is reasonable. Because, the position of the FR-4 sample can be shifted in the course of connecting the sample holder with VNA connectors [11]. The FR-4 sample may be slightly shifted out of the sample holder. Therefore, the true value of L_{01} may be negative.

As illustrated in Table 1, the initial guess is a drawback. The influence of the initial value on the amplitude-only

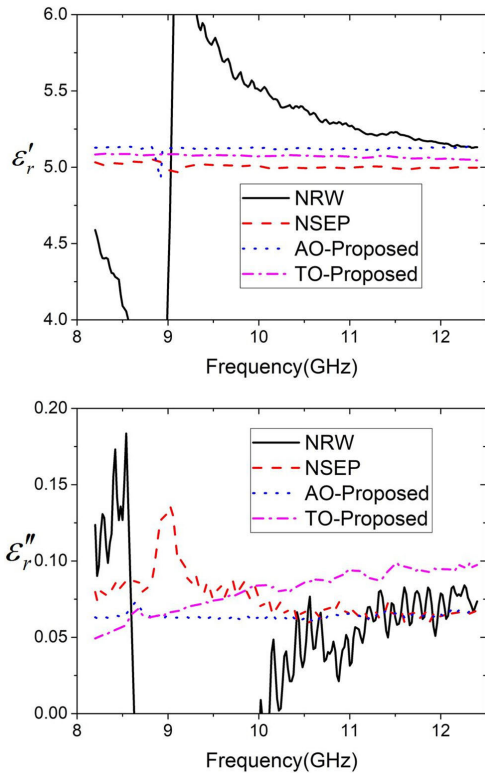


FIGURE 8. Comparison of extracted parameters for the FR-4 using the NRW method [6], the NSEP method [9], the two proposed methods.

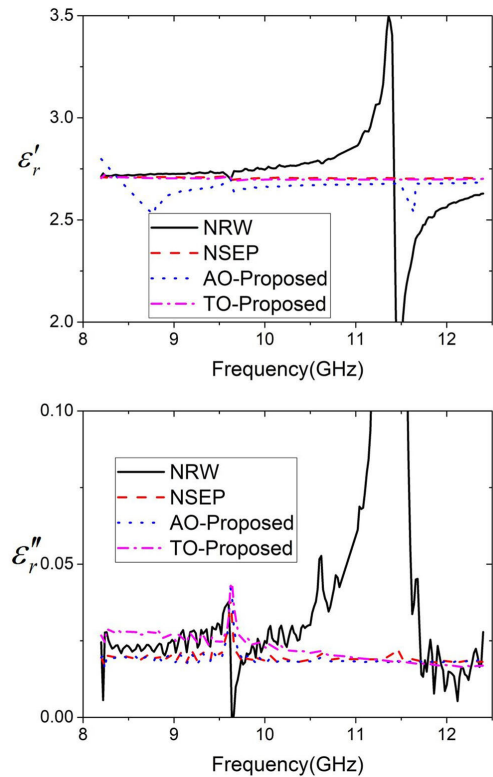


FIGURE 9. Comparison of extracted parameters for the PVC using the NRW method [6], the NSEP method [9], the two proposed methods.

NLSTF is presented in Fig. 7. The extracted values are dependent on the initial values. Therefore, it is better to avoid using the methods dependent on the initial values for characterization of unknown materials or propose a method to obtain a good initial value.

In this paper, we process these measured data with the classical NRW method [6], the NESP method [9], the proposed method with the amplitude-only measurements (AO-Proposed), and the proposed method with the transmission-only measurements (TO-Proposed).

The results determined by the four methods are shown in Fig. 8 and Fig. 9. The FR-4 and PVC are relatively low-loss materials, highly affected by the Fabry-Perot frequencies. Therefore, the ϵ_r determined by the NRW method is unstable. We see that the NESP method and the two proposed methods eliminate the resonances.

For the FR-4 sample, the ϵ'_r determined by the NESP method and the ϵ'_r determined by the proposed methods vary from 5.0 to 5.15 as shown in Fig. 8. That is to say, the variation is within 3 percent for the ϵ'_r determined by NESP and the proposed methods. The ϵ''_r determined by the NESP method and the proposed methods are not the same. We see that the ϵ''_r determined by the NESP are unstable and the ϵ''_r determined by the proposed methods are stable. That is to say the proposed method is more stable than the NESP method for ϵ''_r . For the PVC sample, the ϵ'_r determined by the NESP method and the proposed methods with the transmission-only measurements are almost the same. The ϵ'_r

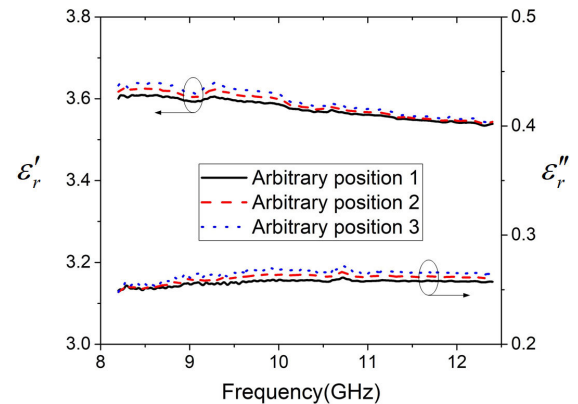


FIGURE 10. Extracted relative complex permittivity for the low-loss sample with different arbitrary positions using the TO-Proposed method.

TABLE 3. True, assumed and estimated positions of the fictional sample.

| Simulation | Ture value | | Assumed value | | Estimated value | |
|------------|---------------|---------------|---------------|---------------|-----------------|---------------|
| | L_{01} (mm) | L_{02} (mm) | L_{01} (mm) | L_{02} (mm) | L_{01} (mm) | L_{02} (mm) |
| 1 | 0.1 | 2.18 | 0 | 2.28 | 0.1 | 2.18 |
| 2 | 1 | 1.28 | 0 | 2.28 | 1.05 | 1.23 |

determined by the proposed method with the amplitude-only measurements fluctuate at some frequency points. The ϵ''_r determined by the NESP method and the proposed methods are almost the same. We can see that the proposed method with the transmission-only measurements is the most stable.

The experiments of a same sample with different positions are used to further validate the proposed method. A low-loss

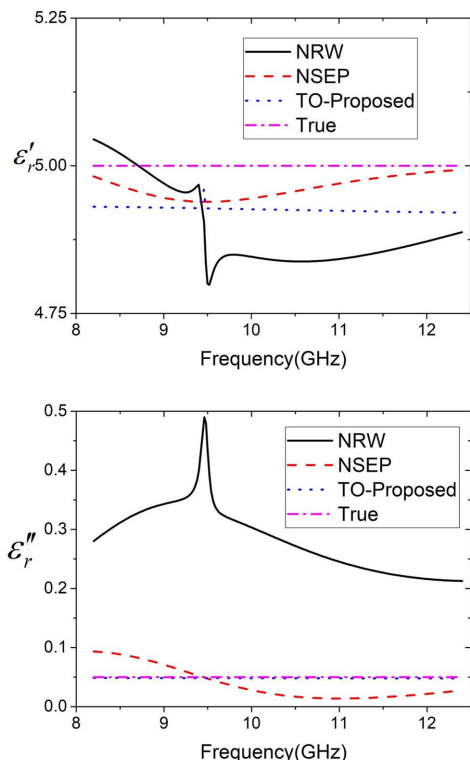


FIGURE 11. Comparison of extracted parameters for the simulated sample with 0.1 mm thicknesses air-gap using the NRW method [6], the NSEP method [9], the TO-Proposed method.

material with thickness of 6.08 mm is fabricated and measured. The material is measured with three arbitrary positions. The ϵ_r extracted by the proposed method (TO) are almost the same as shown in Fig. 10.

IV. SIMULATIONS AND RESULTS

In order to compare the determined ϵ_r with the “true” value to verify the accuracy of the proposed method, we create a frequency-independent material sample and model it in the commercial finite element electromagnetics software, i.e., High Frequency Structure Simulator (HFSS) [10].

The relative complex permittivity of the material sample is defined as $\epsilon_r = 5-j0.05$. The thickness of the sample is 7.5mm and the sample holder is 9.78mm. The three-dimensional geometry in the HFSS contains finite air gaps between the wave ports and the sample surfaces, necessary to model the gaps. This type of air-gap uncertainty is handled in the experimental results as a reference plane position uncertainty [10]. The gap is the position error caused by the displacement [11]. Because, the position of the sample can be shifted in the course of connecting or disconnecting the sample holder with the VNA connectors [11]. In this work, the gap sizes are simulated with thicknesses of 0.1 mm and 1mm.

The techniques in [6], [9] and the proposed method are used to process the simulated S -parameters. For the simulations with the two air-gap, the true, assumed and estimated positions are shown in Table 3. The results verify the accuracy

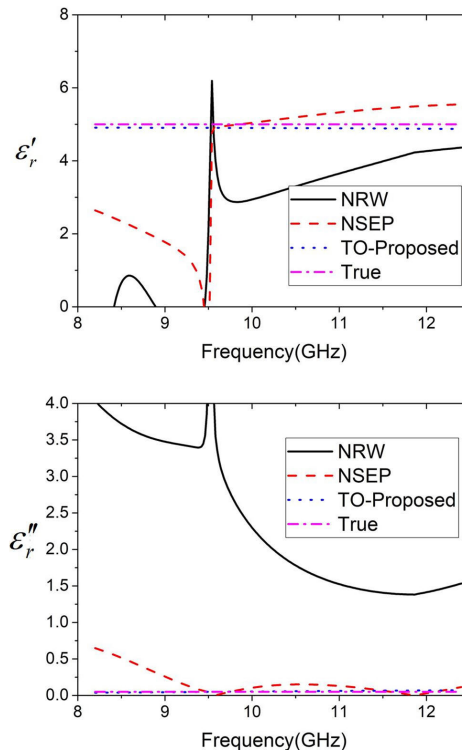


FIGURE 12. Comparison of extracted parameters for the simulated sample with 1 mm thicknesses air-gap using the NRW method [6], the NSEP method [9], the TO-Proposed method.

of the ANN model. For the simulated sample with 1 mm thickness air-gap, the error of the estimated position increases compared with that of the sample with 0.1 mm thickness air-gap. However, the positions for the two simulations are efficiently estimated by the ANN model. Because the ϵ_r extracted by the TO-Proposed method are accurate as shown in Fig. 11 and Fig. 12.

For the simulated sample with 0.1 mm thickness air-gap, the results extracted by the three different methods are shown in Fig. 11. The ϵ_r extracted by the proposed method are close to the true value. For the simulated sample with 1 mm thickness air-gap, the results extracted by the three different methods are shown in Fig. 12. Both of the ϵ'_r and ϵ''_r extracted by the proposed method are close to the true values while the ϵ_r extracted by other methods are far away from the true values. That is to say, the proposed method can obtain more accurate ϵ_r than the other methods especially when the positions of the materials are incorrect. The inaccuracy is caused by the placement shift as illustrated in [11].

V. CONCLUSION

A novel method to determine unique and stable ϵ_r of low-loss materials from the TR measurements has been proposed. The proposed method can eliminate the three drawbacks of the TR measurements by using the simple calculations. The proposed method is important for the TR measurements especially when the position of the sample is unknown or inaccurate.

The proposed method is suitable for material characterization in the terahertz frequency range.

ACKNOWLEDGMENT

The authors would like to thank Dr. Feng Feng from Carleton University, Ottawa, Canada for teaching of the ANN model.

REFERENCES

- [1] L. F. Chen, C. K. Ong, C. P. Neo, V. V. Varadan, and V. K. Varadan, *Microwave Electronics: Measurement and Materials Characterization*. West Sussex, U.K.: Wiley, 2004.
- [2] J. Ma, "The challenging of radio access technology for 5G," in *IEEE MTT-S Int. Microw. Symp. Dig.*, Guangzhou, China, May 2019, pp. 1–4.
- [3] J. Baker-Jarvis, "Transmission/reflection and short-circuit line permittivity measurements," NIST, Gaithersburg, MD, USA, Tech. Note 1341, 1990.
- [4] J. Baker-Jarvis, M. D. Janezic, J. H. Grosvenor, Jr., and R. G. Geyer, "Transmission/reflection and short-circuit line methods for measuring permittivity and permeability," NIST, Gaithersburg, MD, USA, Tech. Note 1355-R, 1992.
- [5] U. C. Hasar, "Determination of complex permittivity of low-loss samples from position-invariant transmission and shorted-reflection measurements," *IEEE Trans. Microw. Theory Techn.*, vol. 66, no. 2, pp. 1090–1098, Feb. 2018.
- [6] W. B. Weir, "Automatic measurement of complex dielectric constant and permeability at microwave frequencies," *Proc. IEEE*, vol. 62, no. 1, pp. 33–36, Jan. 1974.
- [7] S. Trabelsi, A. W. Kraszewski, and S. O. Nelson, "Phase-shift ambiguity in microwave dielectric properties measurements," *IEEE Trans. Instrum. Meas.*, vol. 49, no. 1, pp. 56–60, Feb. 2000.
- [8] V. V. Varadan and R. Ro, "Unique retrieval of complex permittivity and permeability of dispersive materials from reflection and transmitted fields by enforcing causality," *IEEE Trans. Microw. Theory Techn.*, vol. 55, no. 10, pp. 2224–2230, Oct. 2007.
- [9] A.-H. Boughriet, C. Legrand, and A. Chapoton, "Noniterative stable transmission/reflection method for low-loss material complex permittivity determination," *IEEE Trans. Microw. Theory Techn.*, vol. 45, no. 1, pp. 52–57, Jan. 1997.
- [10] D. A. Houtz, D. Gu, and D. K. Walker, "An improved two-port transmission line permittivity and permeability determination method with shorted sample," *IEEE Trans. Microw. Theory Techn.*, vol. 64, no. 11, pp. 3820–3827, Nov. 2016.
- [11] K. H. Baek, J. C. Chun, and W. S. Park, "A position-insensitive measurement of the permittivity and permeability in coaxial airline," in *43rd ARFTG Conf. Dig.*, San Diego, CA, USA, May 1994, pp. 112–116.
- [12] J. A. R. Ball and B. Horsfield, "Resolving ambiguity in broadband waveguide permittivity measurements on moist materials," *IEEE Trans. Instrum. Meas.*, vol. 47, no. 2, pp. 390–392, Apr. 1998.
- [13] Z. Ma and S. Okamura, "Permittivity determination using amplitudes of transmission and reflection coefficients at microwave frequency," *IEEE Trans. Microw. Theory Techn.*, vol. 47, no. 5, pp. 546–550, May 1999.
- [14] U. C. Hasar, "A fast and accurate amplitude-only transmission-reflection method for complex permittivity determination of lossy materials," *IEEE Trans. Microw. Theory Techn.*, vol. 56, no. 9, pp. 2129–2135, Sep. 2008.
- [15] U. C. Hasar, C. R. Westgate, and M. Ertugrul, "Noniterative permittivity extraction of lossy liquid materials from reflection asymmetric amplitude-only microwave measurements," *IEEE Microw. Wireless Compon. Lett.*, vol. 19, no. 6, pp. 419–421, Jun. 2009.
- [16] Z. Szabo, G.-H. Park, R. Hedge, and E.-P. Li, "A unique extraction of metamaterial parameters based on Kramers–Kronig relationship," *IEEE Trans. Microw. Theory Techn.*, vol. 58, no. 10, pp. 2646–2653, Oct. 2010.
- [17] O. Luukkonen, S. I. Maslovski, and S. A. Tretyakov, "A stepwise Nicolson–Ross–Weir-based material parameter extraction method," *IEEE Antennas Wireless Propag. Lett.*, vol. 10, pp. 1295–1298, 2011.
- [18] U. C. Hasar, J. J. Barroso, C. Sabah, and Y. Kaya, "Resolving phase ambiguity in the inverse problem of reflection-only measurement methods," *Prog. Electromagn. Res.*, vol. 129, pp. 405–420, Apr. 2012.
- [19] S. Kim and J. Baker-Jarvis, "An approximate approach to determining the permittivity and permeability near $\lambda/2$ resonances in transmission/reflection measurements," *Prog. Electromagn. Res. B*, vol. 58, pp. 95–109, Mar. 2014.
- [20] S. Kim and J. R. Guerrieri, "Low-loss complex permittivity and permeability determination in transmission/reflection measurements with time-domain smoothing," *Prog. Electromagn. Res. M*, vol. 44, pp. 69–79, Dec. 2015.
- [21] J. Baker-Jarvis, E. J. Vanzura, and W. A. Kissick, "Improved technique for determining complex permittivity with the transmission/reflection method," *IEEE Trans. Microw. Theory Techn.*, vol. 38, no. 8, pp. 1096–1103, Aug. 1990.
- [22] J. Baker-Jarvis, R. G. Geyer, and P. D. Domich, "A nonlinear least-squares solution with causality constraints applied to transmission line permittivity and permeability determination," *IEEE Trans. Instrum. Meas.*, vol. 41, no. 5, pp. 646–652, Oct. 1992.
- [23] U. C. Hasar and O. E. Inan, "Elimination of the dependency of the calibration plane and the sample thickness from complex permittivity measurements of thin materials," *Microw. Opt. Technol. Lett.*, vol. 51, no. 7, pp. 1642–1646, Jul. 2009.
- [24] K. Chalapat, K. Sarvala, J. Li, and G. S. Paraoanu, "Wideband reference-plane invariant method for measuring electromagnetic parameters of materials," *IEEE Trans. Microw. Theory Techn.*, vol. 57, no. 9, pp. 2257–2267, Sep. 2009.
- [25] U. C. Hasar, Y. Kaya, J. J. Barroso, and M. Ertugrul, "Determination of reference-plane invariant, thickness-independent, and broadband constitutive parameters of thin materials," *IEEE Trans. Microw. Theory Techn.*, vol. 63, no. 7, pp. 2313–2321, Jul. 2015.
- [26] U. C. Hasar, "Two novel amplitude-only methods for complex permittivity determination of medium- and low-loss materials," *Meas. Sci. Technol.*, vol. 19, no. 5, Apr. 2008, Art. no. 055706.
- [27] U. C. Hasar, "Unique retrieval of complex permittivity of low-loss dielectric materials from transmission-only measurements," *IEEE Geosci. Remote Sens. Lett.*, vol. 8, no. 3, pp. 562–564, May 2011.
- [28] X. Hao, L. Weijun, and G. Qiulai, "A new dual-channel measurement method for accurate characterization of low-permittivity and low-loss materials," *IEEE Trans. Instrum. Meas.*, vol. 67, no. 6, pp. 1370–1379, Jun. 2018.
- [29] F. Feng, C. Zhang, J. Ma, and Q.-J. Zhang, "Parametric modeling of EM behavior of microwave components using combined neural networks and pole-residue-based transfer functions," *IEEE Trans. Microw. Theory Techn.*, vol. 64, no. 1, pp. 60–77, Jan. 2016.



CHUANG YANG received the B.S. degree in electronic information science and technology from Chongqing University, Chongqing, China, in 2015. He is currently pursuing the Ph.D. degree in microelectronics and solid-state electronics with Tianjin University, Tianjin, China.

His research interests include characterization of materials at microwaves, millimeter waves, and terahertz frequencies, and reliability of microwave devices and circuits.



HUI HUANG (M'16) received the Ph.D. degree in electromagnetic field and microwave technology from the Beijing Institute of Technology, Beijing, China, in 2014.

He joined the Division of Electronics and Information Technology, National Institute of Metrology (NIM), Beijing, in 2005, where he was an Associate Researcher, in 2012. He was involved in the research and development of microwave S-parameters metrology standards and related its traceability systems with NIM. From 2013 to 2014, he carried out his collaborative research as a Visiting Research Scholar in the area of measurements of millimeter-wave and terahertz S-parameters with the National Physical Laboratory, Middlesex, U.K. He is currently with Xinchun Technology Company Ltd., Beijing. His current research interests include coaxial and metallic waveguide S-parameters measurement in high-frequency, on-wafer S-parameter measurement in high-speed electronics, and material electromagnetic properties measurement.

Dr. Huang is a member of the Automatic RF Techniques Group and the IEEE MTT-S Technical Committee on Microwave Measurements (MTT-11).

• • •